Diabetic Hyperglycemia activates CaMKII and Arrhythmias by O linked Glycosylation

Jeffrey R. Erickson[1,2], **Laetitia Pereira**[1], **Lianguo Wang**[1], **Guanghui Han**[3], **Amanda Ferguson**[1], **Khanha Dao**[1], **Ronald J. Copeland**[3], **Florin Despa**[1,4], **Gerald W. Hart**[3], **Crystal M. Ripplinger**[1], and **Donald M. Bers**[1,†]

[1]Department of Pharmacology, University of California, Davis, 451 Health Sciences Drive, Davis, CA 95616 [2]Department of Physiology, University of Otago, Dunedin 9054, New Zealand [3]Department of Biological Chemistry, Johns Hopkins University School of Medicine, 725 North Wolfe St., Baltimore, MD 21205 [4]Department of Molecular and Biomedical Pharmacology, University of Kentucky, 900 S. Limestone, Lexington, KY 40536

Summary

Ca^{2+}-Calmodulin dependent protein kinase II (CaMKII) is a regulatory node in heart and brain, and its chronic activation can be pathological. CaMKII activation seen in heart failure can directly induce pathological changes in ion channels, Ca^{2+} handling and gene transcription.[1] Here we discover a novel mechanism linking CaMKII and hyperglycemic signaling in diabetes mellitus, which is a key risk factor for heart[2] and neurodegenerative diseases.[3,4] Acute hyperglycemia causes covalent modification of CaMKII by O-linked N-acetylglucosamine (O-GlcNAc). O-GlcNAc modification of CaMKII at Ser-279 activates CaMKII autonomously, creating molecular memory even after $[Ca^{2+}]$ declines. O-GlcNAc modified CaMKII is increased in heart and brain from diabetic humans and rats. In cardiomyocytes, increased [glucose] significantly enhances CaMKII-dependent activation of spontaneous sarcoplasmic reticulum (SR) Ca^{2+} release events that can contribute to cardiac mechanical dysfunction and arrhythmias.[1] These effects were prevented by pharmacological inhibition of O-GlcNAc signaling or genetic ablation of CaMKIIδ. In intact perfused hearts, arrhythmias were enhanced by increased [glucose] via O-GlcNAc-and CaMKII-dependent pathways. In diabetic animals, acute blockade of O-GlcNAc inhibited arrhythmogenesis. Thus, O-GlcNAc modification of CaMKII is a novel signaling event in pathways that may contribute critically to cardiac and neuronal pathophysiology in diabetes and other diseases.

†Correspondence to: Donald M. Bers, Ph.D., Department of Pharmacology, University of California, Davis, Genome Building Rm 3513, Davis, CA 95616-8636, Phone: 530-752-6517, Fax: 530-752-7710, dmbers@ucdavis.edu.

Under basal conditions, CaMKII is autoinhibited by interaction between regulatory and catalytic subunits of each CaMKII monomer (Fig 1a). Ca^{2+}/calmodulin (Ca/CaM) binding to the regulatory domain disrupts autoinhibition, opening the structure to allow the catalytic domain to phosphorylate targets.[5] This conformational change is also the basis for fluorescence resonance energy transfer (FRET) changes in a CaMKII activity reporter (Camui), which uses full length CaMKII and attached GFPs (Fig 1a).[6,7] Open-state CaMKII is subject to post-translational modifications, including phosphorylation at T286[8] and oxidation at the MM280/281 pair[9], which stabilize CaMKII in the open-state even when Ca/CaM dissociates, creating molecular memory but also potentially pathological effects.[1] We tested whether diabetic hyperglycemia might alter CaMKII activity.

Using Camui as a direct CaMKII activity reporter, cells exposed to glucose-free or low glucose (100 mg/dL) conditions did not exhibit autonomous CaMKII activity (in lysates $+Ca^{2+}$/CaM/EGTA) (Fig 1b, white bars). However, glucose levels corresponding to borderline or severe diabetes (240–500 mg/dL) induced robust autonomous CaMKII activation. The nonmetabolizable sugar mannitol did not activate autonomous CaMKII activity (Suppl Fig 1a). Glucose-dependent CaMKII activation was still present in CaMKII mutants lacking critical auto-phosphorylation and oxidation sites (Suppl Fig 1b–c), ruling out involvement of those pathways.

Post-translational modification by O-GlcNAc ("O-GlcNAcylation") can alter protein function,[10] and such regulation is seen in heart[11,12] and brain proteins.[13–15] O-GlcNAcylation is enhanced by elevated [glucose] which raises levels of the direct substrate (UDP-N-Acetylglucosamine) of the enzyme O-GlcNAc transferase (OGT; Fig 4g). O-GlcNAc groups are removed by the enzyme O-GlcNAcase. We tested whether direct O-GlcNAcylation might mediate glucose-induced autonomous CaMKII activation, analogous to autophosphorylation in the conserved CaMKII regulatory domain (Suppl Fig 1e). Two consensus O-GlcNAcylation sites are T286 and S279. T286A mutant Camui only slightly limited the glucose-induced autonomous activation (Suppl Fig 1b), but that could be indirect via synergy between O-GlcNAcylation at another site enhancing T286 autophosphorylation.

Remarkably, S279A mutant Camui abolished glucose-induced autonomous CaMKII activation (Fig 1b, black bars). Importantly, S279A had no effect on either direct CaMKII activation or on autonomous activity induced by autophosphorylation or oxidation (Fig 1c). Thus S279 may be a specific target for O-GlcNAc mediated CaMKII activity during hyperglycemia.

High [glucose] did not alter CaMKII activation state in cells kept in Ca^{2+}-free/EGTA conditions (Fig 1d). When cells were exposed to elevated glucose (and normal Ca^{2+}) the subsequently measured maximal Ca^{2+}/CaM-dependent activity was enhanced (middle bars). Pretreatment with the CaMKII inhibitor KN93 (which locks CaMKII in the closed high-FRET state) prevented autonomous activation by high glucose, even in the presence of Ca^{2+}/CaM. Rat cardiomyocytes expressing Camui and exposed to high [glucose] (without stimulation) for 24 hours exhibited no significant change in baseline CaMKII activation vs. low glucose myocytes (Fig 1e). However, increased intracellular $[Ca^{2+}]$, either by pacing (0.5 Hz for 30 s) or isoproterenol (Iso, 100 nM for 20 min) yielded significantly greater

CaMKII activation at higher [glucose]. These observations suggest that O-GlcNAcylation of CaMKII is analogous to autophosphorylation and oxidation, requiring initial opening via Ca^{2+}/CaM.

To confirm our Camui observations, we cultured rat myocytes for 24 hours in varying [glucose] and measured autonomous CaMKII activity (+/− Iso) using a standard assay (^{32}P incorporation into a CaMKII substrate; Fig 1f). CaMKII activity was increased by [glucose]>200 mg/dL, and by both isoproterenol and increased [glucose]. O-GlcNAcylation is dynamic in cells and limited by glucose availability[10] and enzymatic functions of OGT[16] and O-GlcNAcase.[17] Specific inhibition of glutamine:fructose amidotransferase by 50 μM DON (diazo-5-oxonorleucine) to prevent production of the OGT substrate (Fig 4g), and hence O-GlcNAcylation, abolished glucose-induced autonomous CaMKII activation (Fig 1g). Conversely, inhibition of O-GlcNAcase with 100 nM thiamet-G (Thm-G) promotes O-GlcNAc modification and enhanced myocyte CaMKII activity in elevated [glucose]. Mutant Camui S279A was not appreciably activated by high glucose in intact cells (Suppl Fig 1d). Thus, glucose-induced CaMKII activity involves S279 and an O-GlcNAc dependent pathway.

To determine the extent of CaMKII O-GlcNAcylation in heart and brain, we used a custom-designed antibody that specifically recognizes this modification.[15] The fraction of CaMKII that was O-GlcNAc-modified and autophosphorylated were increased in rat myocytes cultured in high vs. normal glucose (350 vs. 150 mg/dL, Fig 2a), confirming that high [glucose] induces O-GlcNAc modification and increased activation of CaMKII. O-GlcNAc modification of CaMKII was blocked by KN93 and in the S279A mutant (Fig 2a), while it was enhanced by treating myocytes with 100 nM Iso 20 min before lysis (Suppl Fig 2a). We verified that the antibody reacted specifically to O-GlcNAc by immunoblots before and after β-elimination reactions that specifically cleaves O-linked glycans without protein degrading (Suppl Fig 2b). The O-GlcNAc antibody no longer recognized CaMKII after β-elimination and high [glucose], but CaMKII levels were unaltered. O-GlcNAc modification of CaMKII was also disrupted by 50 μM DON and enhanced by 100 nM Thm-G (Suppl Fig 2c). We subjected peptides encoding the regulatory domain of CaMKII to in vitro labeling with O-GlcNAc transferase and confirmed the S279 site as a target for O-GlcNAc modification using electron-transfer dissociation mass spectrometry (ETD-MS, Suppl Fig 3).

CaMKII expression is increased in patients with heart failure,[18] and elevated CaMKII expression and activity have been implicated in the transition to heart failure.[19,20] Using the O-GlcNAc specific antibody, we probed cardiac samples (holding total CaMKII constant) from patients with heart failure and diabetes (blood glucose >400 mg/dL), alongside failing and non-failing, non-diabetic hearts (blood glucose <200 mg/dL). The fraction of CaMKII that was O-GlcNAc-modified was doubled in heart failure patients and nearly tripled in heart failure patients with diabetes vs. non-failing, non-diabetic hearts (Fig 2b). Similarly, brain samples from patients with diabetes had significantly increased O-GlcNAc-modified CaMKII vs. non-diabetic patients. In a diabetic rat model with reduced insulin secretion and blood glucose >600 mg/dL,[21] CaMKII O-GlcNAcylation was greatly elevated in heart and brain samples vs. control rats (Fig 2c). Interestingly, CaMKII autophosphorylation was also enhanced in cardiac tissue from diabetic rats (Suppl Fig 2d), consistent with synergistic

CaMKII activation by these mechanisms. Taken together, our data demonstrate that CaMKII O-GlcNAcylation and activation occurs in the heart and brain of diabetic subjects.

Ryanodine receptor (RyR) phosphorylation by CaMKII enhances cardiac SR Ca^{2+} release events (Ca^{2+} sparks and waves).[22–24] In intact isolated myocytes GlcNAcase inhibition with Thm-G or elevated [glucose] alone increased Ca^{2+} spark and wave frequency (Fig 3a–c). The Thm-G-induced Ca^{2+} spark increase occurred without altered SR Ca^{2+} content (Suppl Fig 4a) and was prevented by the CaMKII inhibitor KN-93, but not its inactive analog KN92. Combining Thm-G treatment with increased [glucose] (350 mg/dL) drastically increased Ca^{2+} sparks and waves, consequently depleting SR Ca^{2+} (Suppl Fig 5). Thus, hyperglycemia and reduced GlcNAcase activity synergize in activating SR Ca^{2+} release. Acute blockade of either CaMKII (+KN93) or O-GlcNAcylation (+DON) prevented glucose-dependent Ca^{2+} sparks (Fig 3c), but did not alter SR Ca^{2+} load (Suppl Fig 4b). Control Ca^{2+} spark frequency was neither altered by DON (Fig 3c) nor the nonmetabolizable sugar mannitol (Suppl Fig 4c). Thus, glucose-induced arrhythmogenic Ca^{2+} waves occur through a CaMKII and O-GlcNAc dependent mechanism.

To test whether CaMKIIδ (the dominant cardiac isoform) is required for O-GlcNAc-dependent effects on SR Ca^{2+} release we used myocytes from CaMKIIδ knockout mice (CaMKIIδ-KO). Neither Ca^{2+} transient amplitude nor SR Ca^{2+} load (Suppl Fig 4d,e) were altered by acute Thm-G exposure in wild type (WT) or CaMKIIδ-KO mouse cells. Ca^{2+} spark frequency was significantly enhanced by Thm-G in WT, but not in CaMKIIδ-KO myocytes (Fig 3d).

Using optical mapping in Langendorff perfused rat hearts exposed to 400 mg/dL glucose, we observed a significant increase in premature ventricular complexes (PVCs) vs. baseline (Fig 4a), consistent with observations of enhanced PVCs in human diabetic patients.[25] This effect was attenuated by inhibiting either CaMKII (+KN93) or O-GlcNAc (+DON; Fig 4b). We also mapped $[Ca^{2+}]_i$ and voltage simultaneously. Epicardial activation during PVCs was typified by dramatically slowed conduction and activation time vs. normal activation (Fig 4c). Additionally, spontaneous diastolic Ca^{2+} elevation preceded the action potential upstroke in high glucose (Fig 4d), an effect prevented by blocking OGT by DON pretreatment (Suppl Fig 6a,b).

We also found higher in vivo arrhythmia susceptibility in normal and diabetic rats during caffeine/dobutamine (Caff/DOB) challenge (Fig 4e,f). DON pretreatment ablated arrhythmias induced by Caff/DOB in diabetics, but had no effect on baseline or Caff/DOB induced arrhythmia in non-diabetic rats. We also confirmed that CaMKII activity is elevated in diabetic rat hearts, and this effect is blunted by pretreatment of rats with DON (Suppl Fig 6c), consistent with O-GlcNAc- and CaMKII-dependent hyperglycemia-induced arrhythmogenesis.,

We identified a novel mechanism for autonomous CaMKII activation by O-GlcNAc modification at CaMKII S279 (Fig 4g). Acute extracellular [glucose] elevation to levels that mimic those in diabetic patients suffices to activate CaMKII via this pathway in intact cardiac myocytes and leads to arrhythmic events in intact hearts and animals. In diabetic

hearts and brains CaMKII O-GlcNAcylation is elevated and this may contribute to pathological alterations in cardiac myocytes and neurons. Indeed, this pathway may synergize with autonomous CaMKII activation by phosphorylation[8] and oxidation[26] that is important in signaling in many cell types. The related CaMKIV is O-GlcNAcylated at S189, which inhibits its activation by CaM kinase kinase.[15] O-GlcNAc-mediated activation in CaMKII is not analogous to the inhibition seen for CaMKIV.

The S279 site is highly conserved in all mammalian CaMKII isoforms (Suppl Fig 1e), and the robust functional effects in cardiomyocytes suggest that hyperglycemia can readily activate CaMKII in both heart and brain, and alter phosphorylation of multiple CaMKII targets (including CaMKII itself) to exert both acute (e.g. altered Ca^{2+} handling/ arrhythmias) and chronic (e.g. transcriptional regulation) effects in many tissues. CaMKII is an important nodal point in both acute modulation of ion channels in heart and brain. Over-activation of CaMKII caused by hyperglycemia during diabetes may lead to widespread and as yet unappreciated pathological consequences that merit exploration. It is already known that over-activation of CaMKII occurs in heart failure and neuronal excitotoxicity and that this activated CaMKII can contribute to major dysfunction at the level of acute ion channel modulation that contribute to cardiac arrhythmias,[1,24] reduced contractility, neuronal damage[27] and altered gene transcription.[1] In diabetes, these powerful CaMKII signaling pathways are likely to be activated by hyperglycemia-induced O-GlcNAc modification of CaMKII, and this should be considered in future therapeutic strategies. This could also broaden the impact of CaMKII inhibitors in therapeutics in heart disease and beyond.

METHODS

Construction of Adenoviral Vectors Encoding Biosensors

The Camui construct[7] was incorporated in adenoviruses using the AdEasy™ adenoviral vector system (Qbiogene, Inc., Carlsbad, CA) to ensure high infection efficiency in the terminally differentiated adult ventricular myocytes. Mutant variants of Camui (T286A, CM280/281VV and S279A) were generated using the commercially available QuickChange site directed mutagenesis kit (Stratagene), and likewise incorporated into adenovirus.

HEK293 Cell Transfection

HEK293 cells (mycoplasma free at the time of this study) were cultured in Dulbecco's modified Eagle's medium (Invitrogen) with 5% fetal bovine serum and penicillin/ streptomycin for 24 h and then transiently transfected with expression plasmids encoding Camui using a mammalian transfection kit (Stratagene). Cells were cultured for an additional 36 h post transfection. Camui expression was checked by fluorescence microscopy prior to experiments.

Human and Rat Models of Diabetes

Failing hearts from type 2 diabetic and nondiabetic patients were obtained at the time of orthotopic heart transplantation as a gift from Dr Kenneth Margulies (University of Pennsylvania). Brain samples from human temporal cortex were obtained as a gift from Lee-Way Jin and Mario Melara (University of California, Davis). All human specimens,

including failing heart tissues and brain samples, were obtained in accordance with Institutional Review Board approval at the respective institutions where samples were collected. All tissue was obtained with informed consent prior to transplantation surgery. Inclusion in tissue-based studies was not restricted on the basis of age, sex, race, or ethnic status. Human cardiac tissue samples were divided into three groups: a non-failing and non-diabetic group (Fig 2b **control**; 3 male, 3 female; ages 42–60), a heart failure group not under treatment for diabetes and with blood glucose < 200 mg/dL (**HF**; 3 male, 3 female; ages 41–63), and a heart failure group with diagnosed diabetes and blood glucose > 200 mg/dL (**HF/Diabetes**; 4 male, 2 female; ages 38–66). Human brain tissue samples were divided into two groups: a non-diabetic group (Fig 2b **control**; 3 female; ages 79–89), and a diabetic group with blood glucose > 200 mg/dL (Fig 2b **Diabetes**; 3 female, ages 65–82). Male Sprague-Dawley (SD) rats transgenic for human amylin in the pancreatic β-cells (HIP rats) were used at age 10–12 months as previously described.[28] Animal studies were not randomized or blinded for this study. Sample sizes were determined by power analysis or based on previous studies with the selected models.[28] Blood glucose levels were measured one day before sacrifice using a OneTouch Ultra glucose meter (LifeScan, Inc. Model# AW 060-213-01A). All diabetic HIP rats had a blood glucose concentration of over 600 mg/dL at the time of sacrifice.

In Vitro Fluorescence and CaMKII activity assays

Fluorescence measurements were performed using a MS SpectraMax plate reader spectrophotometer (Molecular Devices). Excitation and emission slits were set at 4 nm. Excitation wavelength of 440 nm was used, and dual photon counting emission detectors were set at 477 nm (F_{CFP}) and 527 nm (F_{YFP}), respectively. HEK cells or rat ventricular myocytes expressing Camui were treated with 10 μM CaM and 200 μM Ca^{2+}, then lysed in a buffer containing 50 mM Tris-HCl (pH 7.5), 5 mM $MgCl_2$, and protease inhibitors to measure "direct" activation (ex. Fig 1b). For autonomous Camui fluorescence measurements, Ca^{2+}/CaM treatment was performed in the presence of 100–500 mg/dL glucose (Fig 1b,d,e,g), 100 μM ATP (Fig 1c), or 1 μM H_2O_2 (Fig 1c). Cell lysis was then performed in a buffer containing 1 mM EGTA to chelate Ca^{2+} and isolate the kinase activity attributed to autonomous (rather than direct) activation. In Fig 1d, cells were pretreated with 1 mM EGTA or 10 μM KN92/KN93. In Fig 1e, myocytes were not directly treated with Ca^{2+}/CaM, but instead were subjected to pacing (0.5 Hz) or treated with Iso (100 nM) in the presence of 100 or 240 mg/dL glucose. In Fig 1g, cells were treated with Ca^{2+}/CaM and increasing [glucose] in the presence of either 50 μM DON or 100 nM Thm-G. In Fig 1f, CaMKII kinase activity was determined at increasing [glucose] and in the presence (and absence) of Iso using a kinase assay that measures incorporation of ^{32}P-ATP into an artificial substrate, syntide-2, as previously described (Fig 1f).[9]

ETD MS Analysis

The peptide was analyzed using an LTQ-Orbitrap XL mass spectrometer (Thermo Fisher Scientific) with electron transfer dissociation (ETD). The synthetic peptide was O-GlcNAcylated by in vitro labeling with OGT overnight at 4 °C. After the O-GlcNAcylation reaction, the pH was adjusted to approximately 3 using 10% formic acid and the sample was desalted with a C18 spin column (The Nest Group, Inc.). The desalted sample was

lyophilized to dryness using a Speed Vac concentrator and re-constituted in 50% methanol, 0.2% acetic acid to a final concentration of 10 pmol/μl. The sample was directly infused into the LTQ-Orbitrap XL mass spectrometer at a flow rate of 1 μl/min using a spray voltage of 1.9 kV. The full MS scans were acquired in the FT analyzer with the following parameters: resolution 100,000; mass scan range (m/z) 300–800; and microscans 1. The ETD MS2 scans were acquired in the ion trap analyzer with the following parameters: reagent AGC target 4E +05; mass scan range (m/z) 250–2000; microscans 1; isolation width (m/z) 1; and ETD activation time 80ms.

Myocyte Isolation and Adenoviral Infection

All protocols involving animals were performed in accordance with the Guide for the Care and Use of Laboratory Animals and approved by the University of California, Davis Institutional Animal Care and Use Committee. Adult rat ventricular myocytes were isolated as previously described.[22] Myocytes were seeded on laminin-coated coverslips in serum-free PC-1 medium (Lonza) supplemented with penicillin/streptomycin. Myocytes were infected for 2 hours at multiplicity of infection of 10–100 with adenovirus encoding Camui, followed by replacement with fresh medium. Infected cells were kept in culture for 36 hours with one final replacement of fresh medium 1 hr before experiments.

Confocal Microscopy Imaging

Cover slips were mounted on the stage of an inverted microscope (Zeiss, LSM5 Pascal) equipped with a 40× 1.4 NA water immersion objective lens. Argon laser excitation wavelengths were 458 nm for CFP and 514 nm for YFP. CFP emission fluorescence was measured by confocal microscopy at 485 ± 15 nm, while YFP emitted fluorescence was measured at ≳535 nm. Camui imaging experiments were performed as previously described.[7] Image-J software was used for image analysis.

Spark Measurements

Intact ventricular myocytes were loaded with Fluo-3 AM (5 μM, Molecular Probes) and transients were recorded as previously described.[29] Ca^{2+} transients were obtained by field stimulation at 1 Hz. SR Ca^{2+} load was evaluated by Ca^{2+} transient upon rapid caffeine application (10 mM). Experiments were performed on confocal microscopy (BioRad, Radiance 2100, 40× objective) using line scan mode with argon 4 laser (λex 488 nm, λem >505 nm). Image analysis used ImageJ software and homemade routines in IDL (interactive data language).

Langendorff perfused rat hearts

All procedures involving animals were approved by the Animal Care and Use Committee of the University of California, Davis and adhered to the Guide for the Care and Use of Laboratory Animals published by the National Institutes of Health. Adult male Sprague-Dawley rats (250–300 g) were anesthetized with pentobarbital sodium (150 mg/kg, IP) containing 500 IU/kg of heparin. Following a midsternal incision, hearts were rapidly excised and Langendorff-perfused at 37°C with oxygenated (95% O_2, 5% CO_2) modified Tyrode's solution of the following composition (in mmol/L): NaCl 128.2, CaCl$_2$ 1.3, KCl

4.7, $MgCl_2$ 1.05, NaH_2PO_4 1.19, $NaHCO_3$ 20 and glucose 11.1 (pH 7.4). Flow rate (6–15 mL/min) was adjusted to maintain a perfusion pressure of 60–70 mmHg. One leaflet of the mitral valve was carefully damaged with sharp forceps inserted through the pulmonary vein to prevent solution congestion in the left ventricular (LV) cavity after suppression of ventricular contraction. This also prevented acidification of the perfusate and the development of ischemia in the LV. Two Ag/AgCl disc electrodes were positioned in the bath to record an electrocardiogram (ECG) analogous to a lead I configuration. ECG was continuously recorded throughout the duration of the experiment. A bipolar pacing electrode was positioned on the base of the LV epicardium for pacing, which was performed at a basic cycle length (BCL) of 200 ms using a 2 ms pulse width at twice the diastolic threshold.

Dual optical mapping of V_m and Ca^{2+}

Hearts were loaded with the fluorescent intracellular Ca^{2+} indicator Rhod-2 AM (Molecular Probes, Eugene, OR; 250 μL of 1mg/mL in dimethyl sulfoxide [DMSO] containing 10% pluronic acid) and were subsequently stained with the voltage-sensitive dye RH237 (Molecular Probes; 25 μL of 1 mg/mL in DMSO). Blebbistatin (Tocris Bioscience, Ellisville, MO; 10–20 μM) was added to the perfusate to eliminate motion artifact during optical recordings. The anterior epicardial surface was excited using LED light sources centered at 530 nm and bandpass filtered from 511–551 nm (LEX-2, SciMedia, Costa Mesa, CA) and focused directly on the surface of the preparation. The emitted fluorescence was collected through a 50mm objective (Nikon, Japan) and split with a dichroic mirror at 630nm (Omega, Brattleboro, VT). The longer wavelength moiety, containing the V_m signal, was longpass filtered at 700 nm and the shorter wavelength moiety, containing the Ca^{2+} signal, was bandpass filtered between 574–606 nm. The emitted fluorescence signals were recorded using two CMOS cameras (MiCam Ultima-L, SciMedia, Costa Mesa, CA) with a sampling rate of 1 kHz and 100×100 pixels with a 20×20 mm field of view. The atrioventricular node was ablated using a fine tip thermal cautery (Acuderm, Ft. Lauderdale, FL) to produce a slow intrinsic rhythm which allowed for ectopic activity and premature ventricular complexes (PVCs) to escape. Following loading of the dyes, baseline electrophysiological parameters were recorded during normal rhythm as well as LV epicardial pacing at a BCL of 200 ms. Hearts were then subjected to hyperglycaemia (400 mg/dL) with (n=3) or without (n=5) pre-treatment (10 min) with the O-GlcNAc inhibitor DON (50 μM). Optical recordings were taken every 5 min following treatment and ECG was continuously recorded.

In vivo ECG recordings

In vivo experiments were performed in anesthetized diabetic rats (blood glucose > 500 mg/ dL). Rats received injection of caffeine (IP; 120 mg/kg) and dobutamine (IV; 50 μg/kg) during in vivo experiments. The same individuals were pre-treated (30 minutes prior to caffeine/dobutamine challenge) with an IP injection of DON (5 mg/kg). Experiments were done one week apart, and some individuals received the reverse of the described procedure (+DON in first trial, -DON in second trial) to control for compensation effects between trials. For quantification of arrhythmia scores, the severity of arrhythmias was quantified using a previously published scoring system.[30] Each individual heart was evaluated by means of a 5-point arrhythmia score, where single PVCs were given a score of 1, bigeminy/

salvos a score of 2, ventricular tachycardia a score of 3, ventricular fibrillation a score of 4, spontaneous ventricular fibrillation a score of 5, and an assigned number corresponded to the most severe type of arrhythmia observed in that heart. Scores were used for group analysis of severity of arrhythmias.

Optical mapping data analysis and statistics

Optical mapping data analysis was performed using two different commercially available analysis programs (BV_Analyze, Brainvision, Tokyo, Japan; and Optiq, Cairn, UK). V_m and Ca^{2+} datasets were spatially aligned and processed with a Gaussian spatial filter (radius 3 pixels). For both action potentials and Ca^{2+} transients (CaTs), activation time was determined as the time at 50% between diastolic and peak amplitude. Diastolic Ca^{2+} elevation was measured as the percentage of diastolic Ca^{2+} increase relative to the following CaT amplitude at baseline and 30 min post-treatment. The average diastolic Ca^{2+} elevation was calculated for each heart by averaging all Ca^{2+} signals from the entire anterior surface of the heart within the optical mapping field of view. PVC incidence was determined from the continuous ECG recording as the number of PVCs that occurred during a 15 min period of baseline activity (before initiation of treatment) and during the first 15 min of treatment.

All values are presented as mean±SEM, *n* values are generally biological replicates (hearts, brains, animals, myocytes, cell preparations) as indicated in legends. In addition, 3 technical replicates (triplicates) from 3 biological replicates were used for some cellular Camui experiments in Fig 1 s. Comparisons between two groups of data were made using a Student's t-test, paired where appropriate. P<0.05 was considered statistically significant.

Supplementary Material

Refer to Web version on PubMed Central for supplementary material.

ACKNOWLEDGEMENTS

REFERENCES

1. Anderson ME, Brown JH, Bers DM. CaMKII in myocardial hypertrophy and heart failure. J Mol Cell Cardiol. 2011; 51:468–473. [PubMed: 21276796]

2. Roger VL, et al. Heart disease and stroke statistics--2011 update: a report from the American Heart Association. Circulation. 2011; 123:e18–e209. [PubMed: 21160056]

3. Haan MN. Therapy Insight: type 2 diabetes mellitus and the risk of late-onset Alzheimer's disease. Nat Clin Pract Neurol. 2006; 2:159–166. [PubMed: 16932542]

4. Biessels GJ, Staekenborg S, Brunner E, Brayne C, Scheltens P. Risk of dementia in diabetes mellitus: a systematic review. Lancet Neurol. 2006; 5:64–74. [PubMed: 16361024]

5. Rosenberg OS, Deindl S, Sung RJ, Nairn AC, Kuriyan J. Structure of the autoinhibited kinase domain of CaMKII and SAXS analysis of the holoenzyme. Cell. 2005; 123:849–860. [PubMed: 16325579]

6. Takao K, Okamoto K, Nakagawa T, Neve RL, Nagai T, Miyawaki A, Hashikawa T, Kobayashi S, Hayashi Y. Visualization of synaptic Ca^{2+}/calmodulin-dependent protein kinase II activity in living neurons. J Neurosci. 2005; 25:3107–3112. [PubMed: 15788767]

7. Erickson JR, Patel R, Ferguson A, Bossuyt J, Bers DM. Fluorescence resonance energy transfer-based sensor Camui provides new insight into mechanisms of calcium/calmodulin-dependent protein kinase II activation in intact cardiomyocytes. Circ Res. 2011; 109:729–738. [PubMed: 21835909]

8. Hudmon A, Schulman H. Structure-function of the multifunctional Ca^{2+}/calmodulin-dependent protein kinase II. Biochem J. 2002; 364:593–611. [PubMed: 11931644]

9. Erickson JR, Joiner ML, Guan X, Kutschke W, Yang J, Oddis CV, Bartlett RK, Lowe JS, O'Donnell SE, Aykin-Burns N, Zimmerman MC, Zimmerman K, Ham AJ, Weiss RM, Spitz DR, Shea MA, Colbran RJ, Mohler PJ, Anderson ME. A dynamic pathway for calcium-independent activation of CaMKII by methionine oxidation. Cell. 2008; 133:462–474. [PubMed: 18455987]

10. Hart GW, Housley MP, Slawson C. Cycling of O-linked beta-N-acetylglucosamine on nucleocytoplasmic proteins. Nature. 2007; 446:1017–1022. [PubMed: 17460662]

11. Chatham JC, Marchase RB. The role of protein O-linked beta-N-acetylglucosamine in mediating cardiac stress responses. Biochim Biophys Acta. 2010; 1800:57–66. [PubMed: 19607882]

12. Zhu-Mauldin X, Marsh SA, Zou L, Marchase RB, Chatham JC. Modification of STIM1 by O-linked N-acetylglucosamine (O-GlcNAc) attenuates store-operated calcium entry in neonatal cardiomyocytes. J Biol Chem. 2012; 287:39094–39106. [PubMed: 22992728]

13. Rengifo J, Gibson CJ, Winkler E, Collin T, Ehrlich BE. Regulation of the inositol 1,4,5-trisphosphate receptor type I by O-GlcNAc glycosylation. J Neurosci. 2007; 27:13813–13821. [PubMed: 18077693]

14. Bimboese P, Gibson CJ, Schmidt S, Xiang W, Ehrlich BE. Isoform-specific regulation of the inositol 1,4,5-trisphosphate receptor by O-linked glycosylation. J Biol Chem. 2011; 286:15688–15697. [PubMed: 21383013]

15. Dias WB, Cheung WD, Wang Z, Hart GW. Regulation of calcium/calmodulin-dependent kinase IV by O-GlcNAc modification. J Biol Chem. 2009; 284:21327–21337. [PubMed: 19506079]

16. Kreppel LK, Blomberg MA, Hart GW. Dynamic glycosylation of nuclear and cytosolic proteins. Cloning and characterization of a unique O-GlcNAc transferase with multiple tetratricopeptide repeats. J Biol Chem. 1997; 272:9308–9315. [PubMed: 9083067]

17. Gao Y, Wells L, Comer FI, Parker GJ, Hart GW. Dynamic O-glycosylation of nuclear and cytosolic proteins: cloning and characterization of a neutral, cytosolic beta-N-acetylglucosaminidase from human brain. J Biol Chem. 2001; 276:9838–9845. [PubMed: 11148210]

18. Hoch B, Meyer R, Hetzer R, Krause EG, Karczewski P. Identification and expression of delta-isoforms of the multifunctional Ca^{2+}/calmodulin-dependent protein kinase in failing and nonfailing human myocardium. Circ Res. 1999; 84:713–721. [PubMed: 10189359]

19. Zhang T, Maier LS, Dalton ND, Miyamoto S, Ross J Jr, Bers DM, Brown JH. The deltaC isoform of CaMKII is activated in cardiac hypertrophy and induces dilated cardiomyopathy and heart failure. Circ Res. 2003; 92:912–919. [PubMed: 12676814]

20. Ling H, Zhang T, Pereira L, Means CK, Cheng H, Gu Y, Dalton ND, Peterson KL, Chen J, Bers D, Brown JH. Requirement for Ca^{2+}/calmodulin-dependent kinase II in the transition from pressure overload-induced cardiac hypertrophy to heart failure in mice. J Clin Invest. 2009; 119:1230–1240. [PubMed: 19381018]

21. Butler AE, Jang J, Gurlo T, Carty MD, Soeller WC, Butler PC. Diabetes due to a progressive defect in beta-cell mass in rats transgenic for human islet amyloid polypeptide (HIP Rat): a new model for type 2 diabetes. Diabetes. 2004; 53:1509–1516. [PubMed: 15161755]

22. Kohlhaas M, Zhang T, Seidler T, Zibrova D, Dybkova N, Steen A, Wagner S, Chen L, Brown JH, Bers DM, Maier LS. Increased sarcoplasmic reticulum calcium leak but unaltered contractility by

acute CaMKII overexpression in isolated rabbit cardiac myocytes. Circ Res. 2006; 98:235–244. [PubMed: 16373600]

23. Guo T, Zhang T, Mestril R, Bers DM. Ca^{2+}/Calmodulin-dependent protein kinase II phosphorylation of ryanodine receptor does affect calcium sparks in mouse ventricular myocytes. Circ Res. 2006; 99:398–406. [PubMed: 16840718]

24. Zhao Z, Fefelova N, Shanmugam M, Bishara P, Babu GJ, Xie LH. Angiotensin II induces afterdepolarizations via reactive oxygen species and calmodulin kinase II signaling. J Mol Cell Cardiol. 2011; 50:128–136. [PubMed: 21059353]

25. DelGobbo LC, Song Y, Poirier P, Dewailly E, Elin RJ, Egeland GM. Low serum magnesium concentrations are associated with a high prevalence of premature ventricular complexes in obese adults with type 2 diabetes. Cardiovasc Diabetol. 2012; 11:23. [PubMed: 22405520]

26. Luo M, Guan X, Luczak ED, Lang D, Kutschke W, Gao Z, Yang J, Glynn P, Sossalla S, Swaminathan PD, Weiss RM, Yang B, Rokita AG, Maier LS, Efimov IR, Hund TJ, Anderson ME. Diabetes increases mortality after myocardial infarction by oxidizing CaMKII. J Clin Invest. 2013; 123:1262–1274. [PubMed: 23426181]

27. Ashpole NM, Hudmon A. Excitotoxic neuroprotection and vulnerability with CaMKII inhibition. Mol Cell Neurosci. 2011; 46:720–730. [PubMed: 21316454]

Methods References

28. Despa S, Margulies KB, Chen L, Knowlton AA, Havel PJ, Taegtmeyer H, Bers DM, Despa F. Hyperamylinemia contributes to cardiac dysfunction in obesity and diabetes: a study in humans and rats. Circ Res. 2012; 110:598–608. [PubMed: 22275486]

29. van Oort RJ, McCauley MD, Dixit SS, Pereira L, Yang Y, Respress JL, Wang Q, De Almeida AC, Skapura DG, Anderson ME, Bers DM, Wehrens XH. Ryanodine receptor phosphorylation by calcium/calmodulin-dependent protein kinase II promotes life-threatening ventricular arrhythmias in mice with heart failure. Circulation. 2010; 122:2669–2679. [PubMed: 21098440]

30. Curtis MJ, Walker MJ. Quantification of arrhythmias using scoring systems: an examination of seven scores in an in vivo model of regional myocardial ischaemia. Cardiovasc Res. 1988; 22:656–665. [PubMed: 3242835]
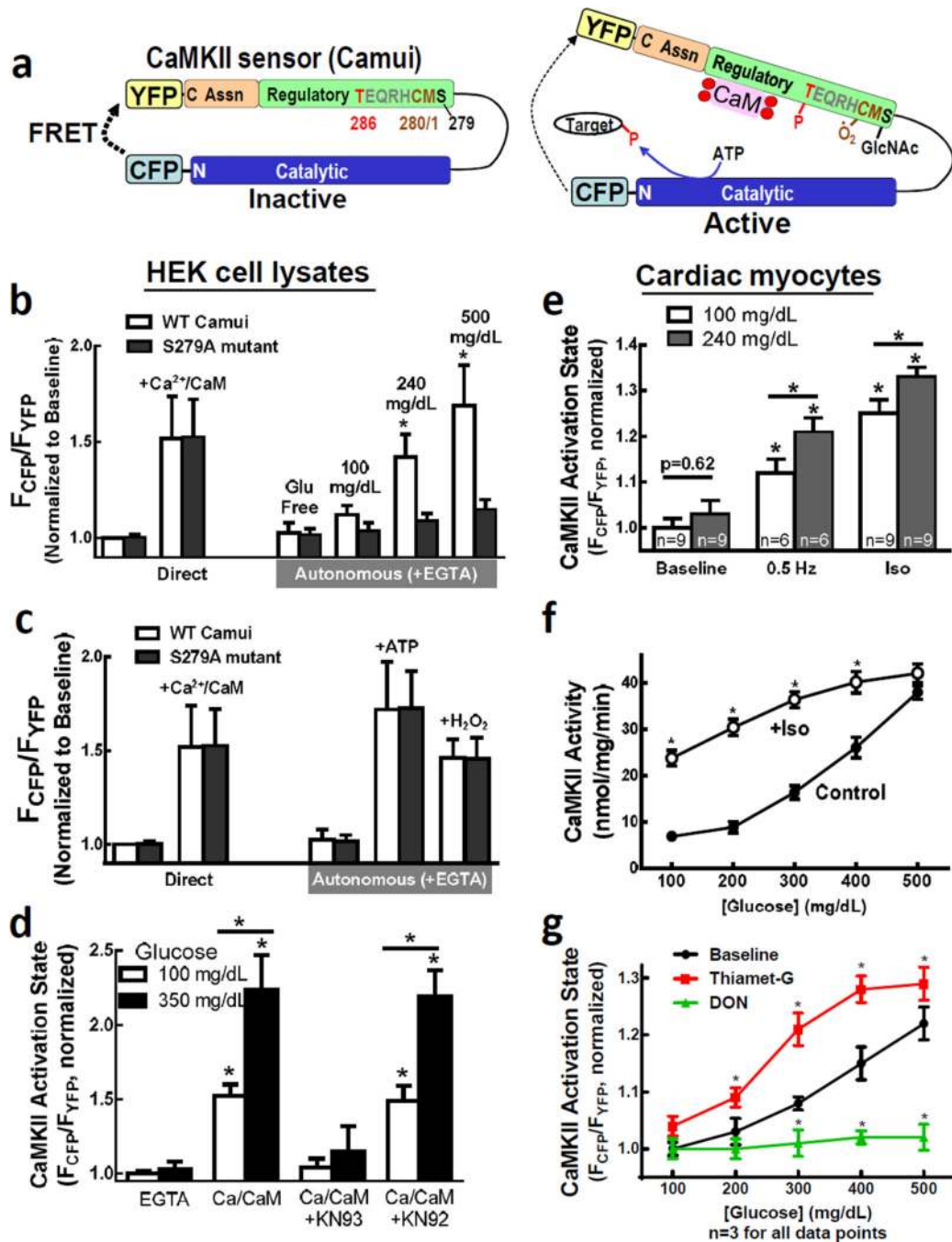
Figure 1. Glucose induced CaMKII activity is O-GlcNAc dependent

a, Schematic of Camui sensor. **b**, Direct (Ca^{2+}/CaM) or autonomous (+EGTA) activation of Camui measured in lysates after HEK cell exposure to indicated [glucose]. **c**, S279 mutation does not affect Ca^{2+}/CaM, phosphorylation, or oxidation-dependent activity. **d**, Glucose-dependent Camui activation is ablated by KN93 or Ca^{2+} chelation (+EGTA). **e**, Increased [glucose] enhances pacing- or Iso-induced CaMKII activity. **f**, Glucose-dependent CaMKII activity measured by ^{32}P incorporation. **g**, Glucose-dependent Camui activation is enhanced

by Thm-G and ablated by O-GlcNAc inhibition (+DON). Mean±s.e.m. 3 preparations × triplicates, unless indicated. * p<0.05 vs. control.
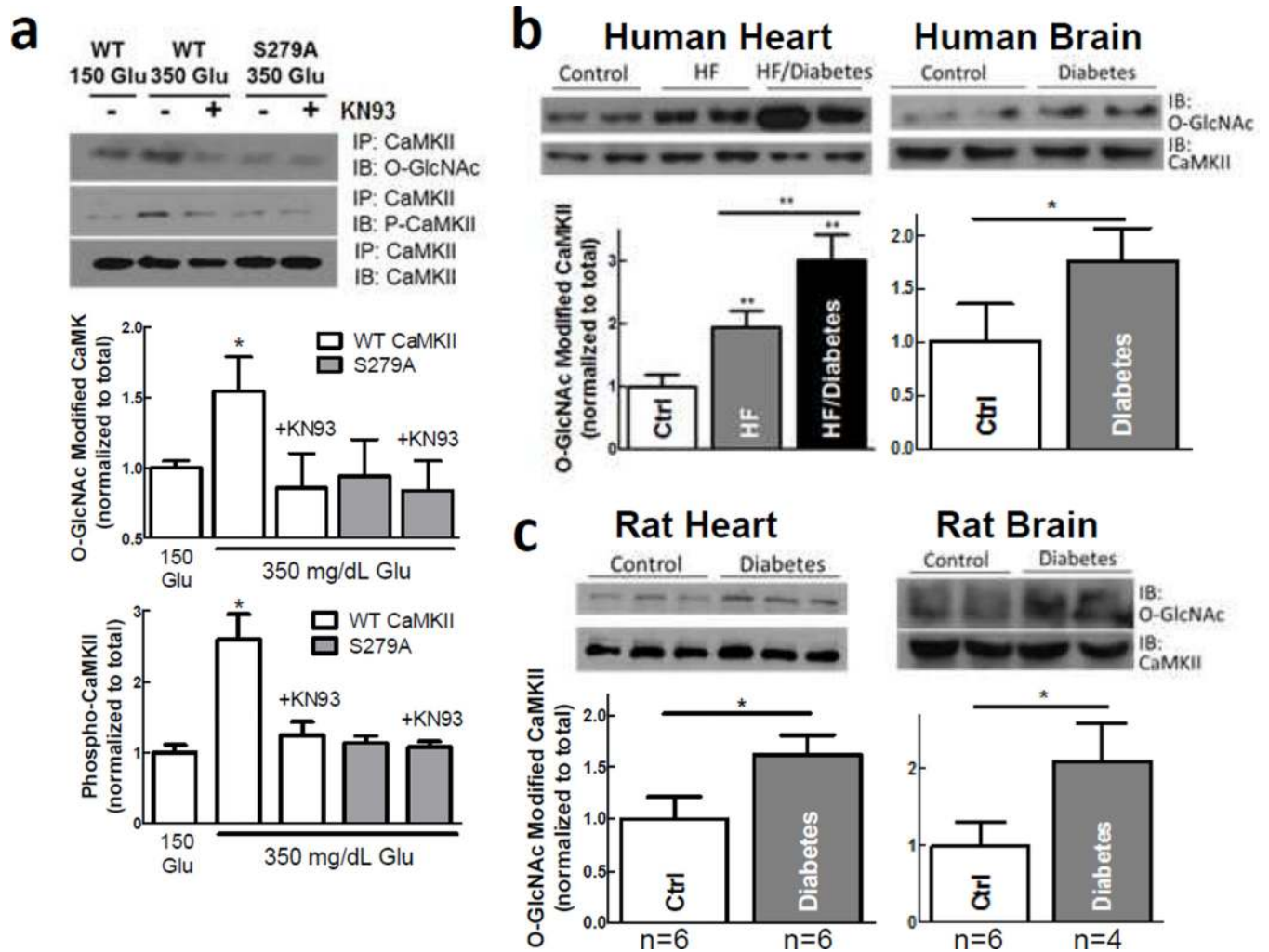
Figure 2. O-GlcNAcylation of CaMKII occurs *in vivo*

a, Immunoblot with O-GlcNAc- and P-T286-specific antibodies shows that high [glucose] increases O-GlcNAcylation and activation of CaMKII, but not in S279A mutant or after KN93 (n=3 myocyte preparations). **b**, The ratio of O-GlcNAc modified to total CaMKII is increased in heart (n=6 hearts/group) and brain (n=3 brains/group) from diabetic vs. control non-diabetic human patients. **c**, O-GlcNAc modification of CaMKII is also increased in heart and brain from diabetic rats compared to wild type controls (number of rats indicated). Mean±s.e.m. * $p<0.05$, ** $p<0.01$ vs. control.
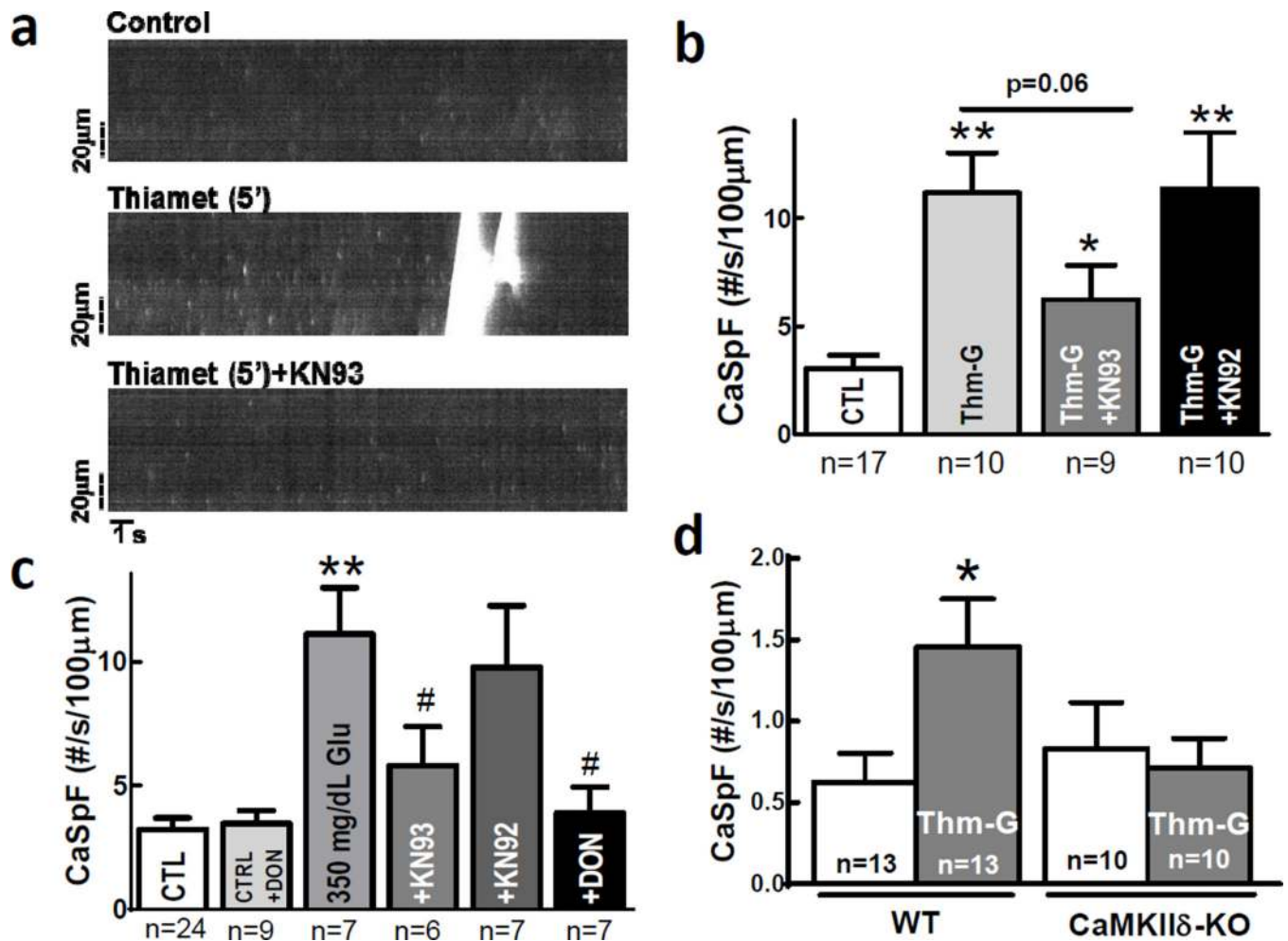
Figure 3. Glucose-induced cardiac Ca^{2+} sparks are O-GlcNAc- and CaMKII-dependent

Ca^{2+} sparks and waves **a**, are increased by GlcNAcase inhibitor Thm-G. **b**, Thm-G-induced Ca^{2+} sparks are prevented by CaMKII inhibitor KN93 (not inactive analog KN92). **c**, Glucose induced Ca^{2+} sparks are ablated by CaMKII inhibitor KN93 and the O-GlcNAc inhibitor DON. # $p<0.05$ vs. 350 mg/dL glucose. **d**, Thm-G induces Ca^{2+} sparks in WT mice, but not mice lacking CaMKIIδ (baseline Ca^{2+} spark frequency differs in rat vs. mouse myocytes). Data are mean±s.e.m. number of myocytes indicated in panels, * $p<0.05$, ** $p<0.01$ vs. control.

Figure 4. Glucose-induced PVCs are suppressed by DON and KN-93

a, ECGs during baseline (top), high [glucose] (HG), and DON pretreatment +HG. **b**, PVCs (/15 min) after HG increased (vs. baseline), while DON or KN93 reduced PVCs only in HG. **c**, Activation maps for normal activation (top) and HG-induced PVC (bottom). **d**, Action potentials (black) and Ca^{2+} transients (red) from area indicated by white boxes in (**c**). **e,f**, Caff/DOB-induced PVCs were inhibited by DON in diabetic rats in vivo. **g**, Working model

of O-GlcNAc-induced and CaMKII-dependent arrhythmic events. Mean±s.e.m. n=3 hearts/animals, * p<0.05 vs. control.